Feasibility Study of On-line Digital X-ray Imaging for Irradiated Fuel Rods

Y. Parthoens*, V. Smolders°, A. Gys*
**Reactor Material Research Department, SCK•CEN, Mol, Belgium*
°Industrial Engineer Department, Katholieke Hogeschool Kempen, Geel, Belgium

Abstract. At the Reactor Material Research Department of the Belgian Nuclear Research Centre SCK•CEN X-ray imaging of the internal parts of irradiated fuel rods is done on silver-halide films using a 420kV X-ray source. The replacement of the films by an on-line digital X-ray imaging system implies several advantages. Images can be evaluated instantly and source parameters can be optimized more easily. Time consuming film development is superfluous. The images can digitally be enhanced, processed, reported and archived. Within this work the feasibility of four commercial on-line digital X-ray imaging systems were studied for post-irradiation examination on fuel rods in a hot cell environment. The criteria to evaluate the systems were image quality, integration in the existing hot cell infrastructure, durability and cost price. For the evaluation and comparison of the image quality a simulation fuel rod was fabricated. Three systems suffered from lack of sensitivity, contrast and/or resolution. Only the CsI-scintillator coupled to a CCD-camera with image intensifier gave a sufficient image quality. On the other hand the image intensifiers' dimensions are difficult to integrate in the existing hot cell infrastructure. Also the durability of intensifier screens is questionable as they are susceptible to image burn. Smaller image intensifiers easier to integrate are commercial available nowadays.

1. Introduction

Conventional X-ray imaging consists of capturing the radiation pattern on individual hardcopies of silver-halide emulsion films. These intrinsic high resolution[1] films are unique copies that need to be viewed on an intense light source. A correct development, handling and archiving is needed in order to preserve the quality of the films. Nevertheless silver-halide films are still used extensively for their high quality in image resolution. The last decade the digitalization of X-ray imaging has found its way through in medical radiological applications where X-ray energies are used up to 150keV. Also other applications like electronic portal imaging devices, to verify the position of a high-energy therapeutic X-ray beam relative to the internal anatomy, X-ray crystallography, for the evaluation of the microscopic three-dimensional structure of crystals and molecules, and non-destructive testing of industrial products are experimenting with digital imaging [4].

The easiest way of digitizing X-ray images is by scanning the films in a film digitizer. A HeNe-laser or Charged Coupled Device (CCD) can be used to determine the optical density[2] of the image with a scan resolution up to 50µm [1]. The film digitizing is interesting for long term archiving purposes and post imaging processing like enhancement [5] and reporting. Figure 1 illustrates the brightness and contrast enhancement of a fuel rod X-ray image scanned with a laser film digitizer. The film digitizer can be implemented for any X-ray application (up to 50µm image resolution[3]) as it only requires the

[1] Resolution or resolving power: the closest seperation of a pair of linear objects at which the images do not merge, expressed in distance between these lines [mm] or in number of lines per unit length [mm^{-1}]. The resolution or resolving power of a final image is determined by different parameters like: type of film or digital detector, sensitivity, contrast, image unsharpness, noise and energy spectrum of X-ray bundle. Typical values range from 0.03mm to 0.5mm [2, 3].

[2] Optical density *D* is defined as*: $log(I_0/I)$* where I_0 is the incident light intensity on the film and I the transmitted light intensity through the film. As the physiological response of the eye is also logaritmic to visible light, the optical density is an accurate representation of the grayscales the eye sees.

[3] There is no gain in image resolution by decreasing the pixel size below the resolving power of the imaging system [2]

initial hardcopy. However, films still have to be developed and no on-line imaging[4] is possible. For departments with a great number of X-ray installations the investment in a film digitizer is an easy and relative cheap solution. On the other hand, the initial investment for a single installation is too high compared to the purchase of a digital X-ray detector.

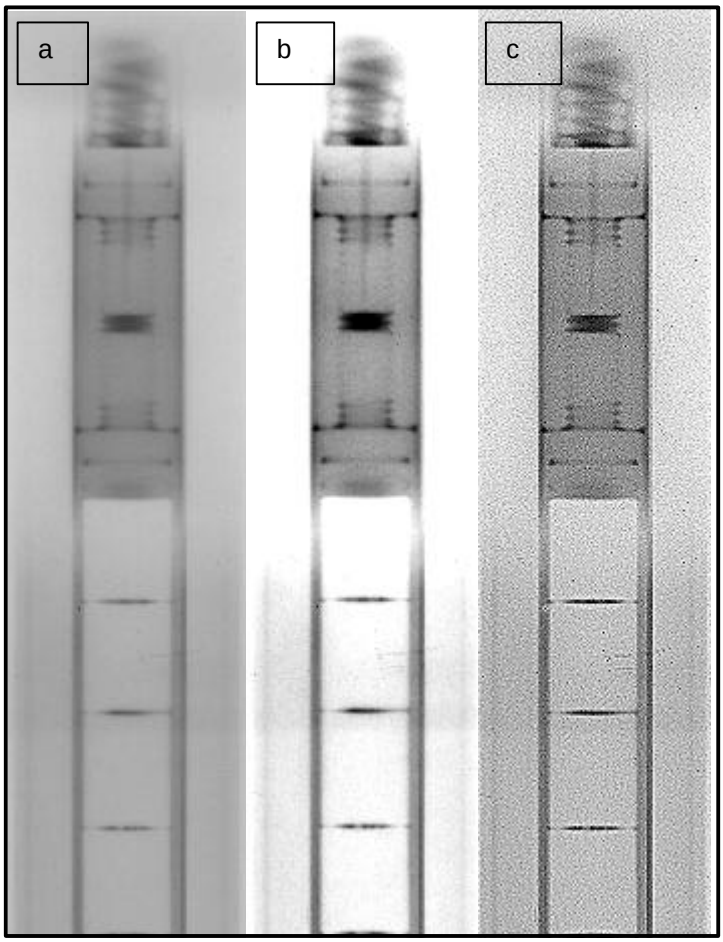

Fig. 1. Image enhancement of an irradiated fuel rod X-ray image digitized with a film digitizer, (a) original digitized image, (b) contrast and brightness enhancement by relevelling the look up table of the grayscales, grayscale values are redistributed in the pixel values of interest, details in the fuel dishes, fuel rod plug and spring are more visible (c) image sharpening using a two dimensional software filter also reveals more detail towards the original image. Care must be taken when using software filters not to introduce any artifacts.

Another off-line method of digitizing X-ray imaging systems is replacing the silver-halide film with a digital X-ray detector. Financial costs for films and development will be non-existent. Especially in case of a high film throughput the investment in a digital detector will be more economical. A first type of digital detectors are storage phosphor computed radiography systems (Figure 2). A special-purpose

[4] On-line imaging is creating a final image which can be viewed within a few seconds after inintializing the X-ray imaging, taking into account the integration time of the system needed to acquire a satisfied image quality. Discreet images can be displayed sequentially in function of time. On the contrary real-time imaging implies a continuos display of images in function of time. Most digital X-ray imaging systems are discrete on-line systems.

screen consisting of photo-stimulatable phosphor like BaFBr0.85I0.15 or BaFX:Eu2+ replaces the silver-halide film [4,6-8]. After exposure the storage phosphor screen is then laser-spot scanned in a reader system to stimulate luminescence proportional to the original X-ray exposure. The luminescence image is detected through a photo-multiplier and converted into a digital image. The image resolution and sensitivity performance of these systems are comparable to coarse grain films[5] or screen-films[6] up to about 250kV tube voltage. On-line imaging is impossible due to the use of a separate screen reader system.

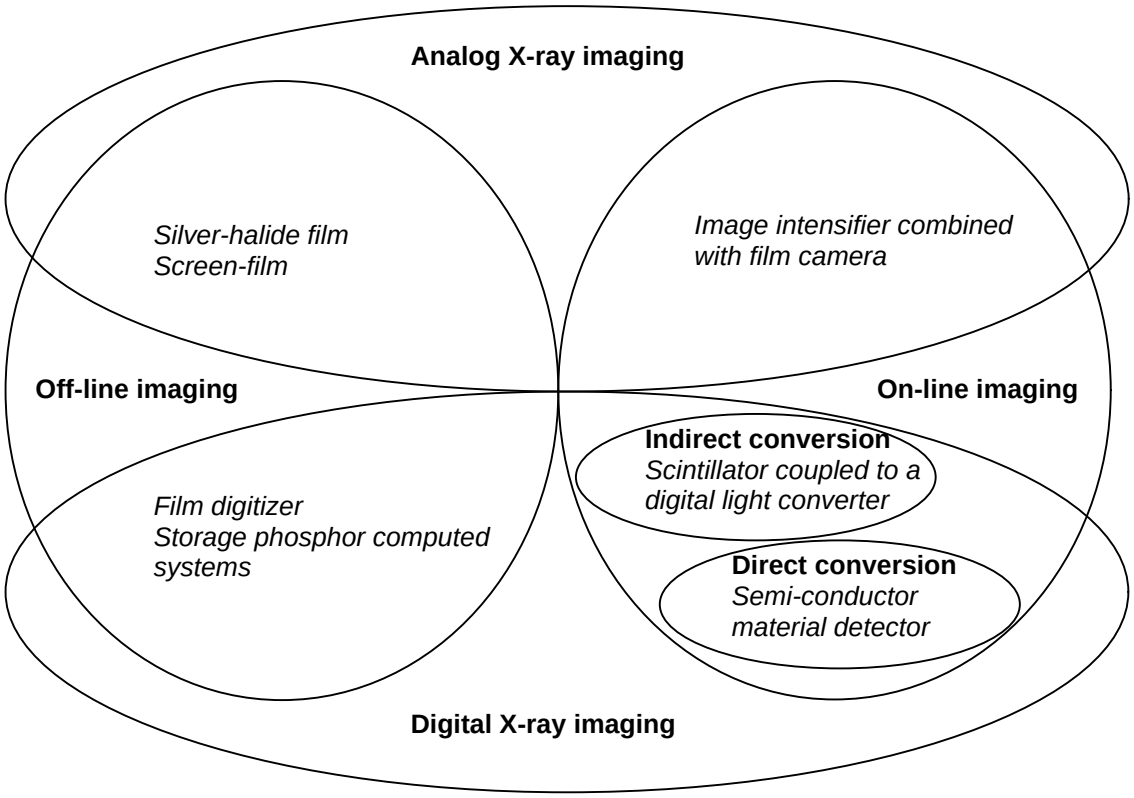

Fig. 2. Schematic overview of X-ray imaging system with examples

On-line digital X-ray detectors can be divided into two categories: indirect- and direct-conversion digital radiography systems (Figure 2, 3, and 4) [4]. The indirect-conversion systems incorporate a scintillator screen to convert the X-rays to light. The light emitted via fluorescence is then absorbed by a detector, such as CCD-cameras and flat panel amorphous-silicon photodiodes, and converted into a digital image [9]. Generally these systems suffer from image resolution versus sensitivity tradeoffs.

[5] Coarse grain film: the resolution and sensitivity of an X-ray film is determined by the size of the silver-halide grains in the emulsion. The larger the grains, the better the sensitivity, but the worser the resolution [2].

[6] Screen-film: an intensifying screen is kept in contact with the film in order to increase the optical density or sensitivity of the film. The fluorescense material in the screen is excited by the X-rays and emits light contributing to the exposure of the film. Also sheets of thin lead may be used in industrial radiography with high X-ray energy applications. In this case, the increased exposure to the film is caused by secondary electrons and characteristic X-ray emitted by the lead initialised by the primary X-rays. The use of an intensifying screen increases the sensitivity but deteriorates the resolution. [2]

Higher energy applications will demand a thicker scintillator to absorb the X-rays in an efficient way, but image resolution will deteriorate due to light scattering in the scintillator. A possible solution is the use of structured scintillators where the absorbed X-ray is confined to a narrow vertical channel, which prevents the light from scattering or spreading sideways (Figure 5). These scintillators have a constant image resolution independent of the thickness of the scintillator. However, even though these structures seem to be an ideal solution, in practice they are difficult and expensive to manufacture and they often have internal absorption and light cross talk mechanisms that can outweigh their advantages.

Direct-conversion digital X-ray detectors employs a material such as selenium, mercuric, iodide, cadmium telluride, lead iodide or an other semiconductor to immediately absorb the incident X-ray and produce electron-hole pairs that can be measured digitally. These direct systems present better resolution as the electron-hole pairs do not disperse laterally, even for the relative thick layers needed to assure good X-ray absorption of high-energy X-rays. Also good noise properties can be achieved with for example amorphous selenium due to its intrinsic low dark current [4]. As mentioned before the indirect- and direct-conversion digital X-ray detectors make on-line imaging possible as sequences of discrete digital images in function of time. The time between two image sequences is determined by the integration time of the digital system needed to acquire a satisfied image quality. Notice that on-line systems are not new and were already available since 1948 [27] as analog real-time systems where images are viewed continuously in function of time. These systems usually involve a television camera combined with an image intensifier and CsI:Tl fluorescent screen [2].

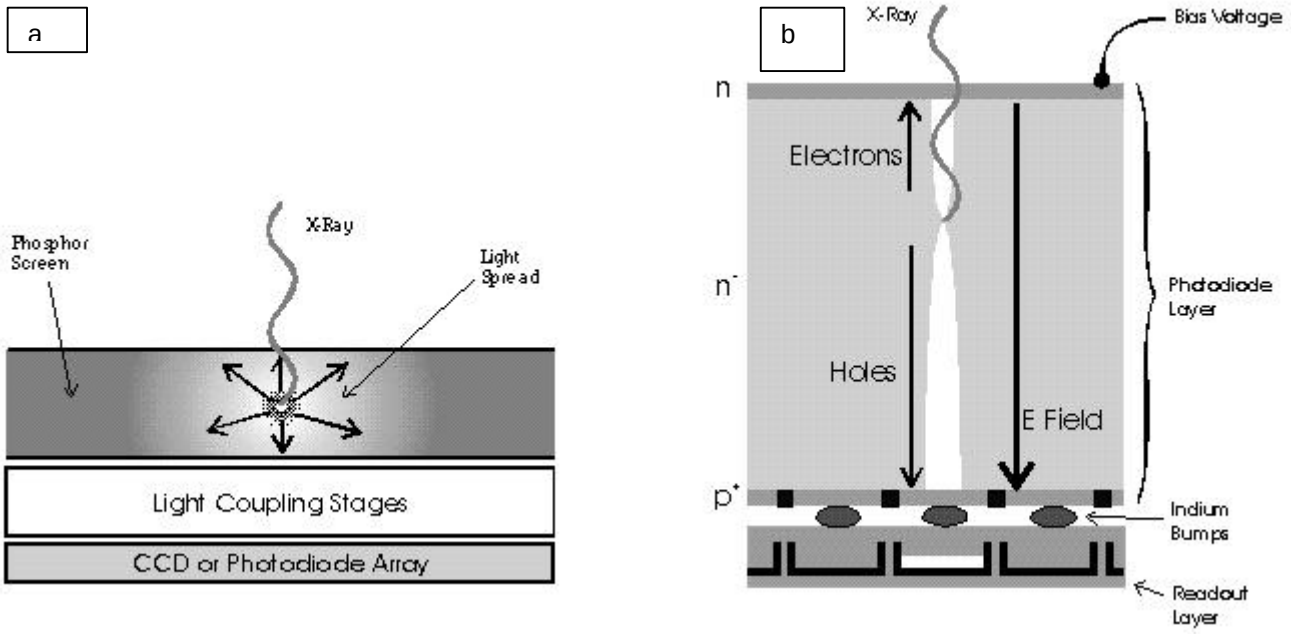

Fig. 3. Schematic view of on-line digital X-rays detectors,
(a) Indirect conversion system, (b) Direct conversion system [11]

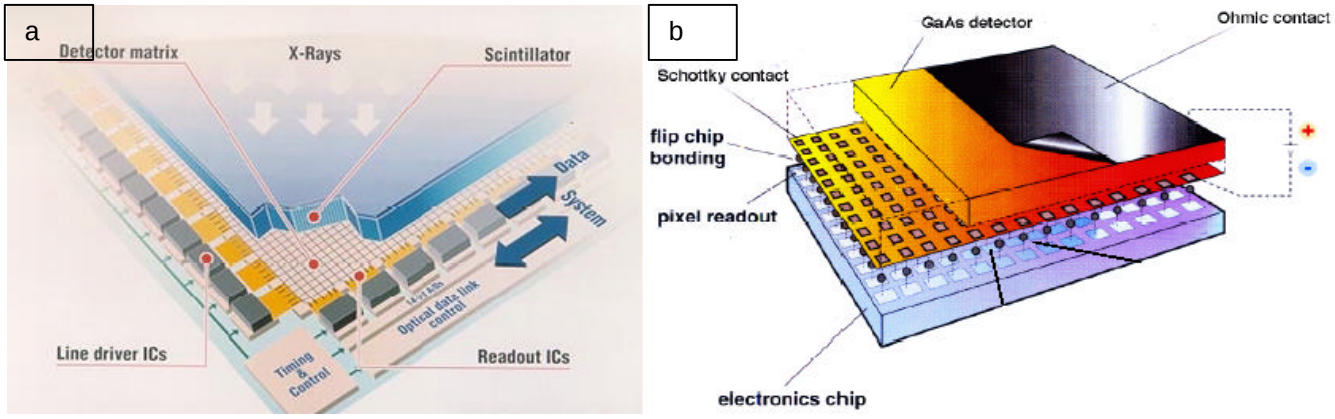

Fig. 4. Design of on-line digital X-rays detectors,
(a) Indirect conversion system, (b) Direct conversion system [12]

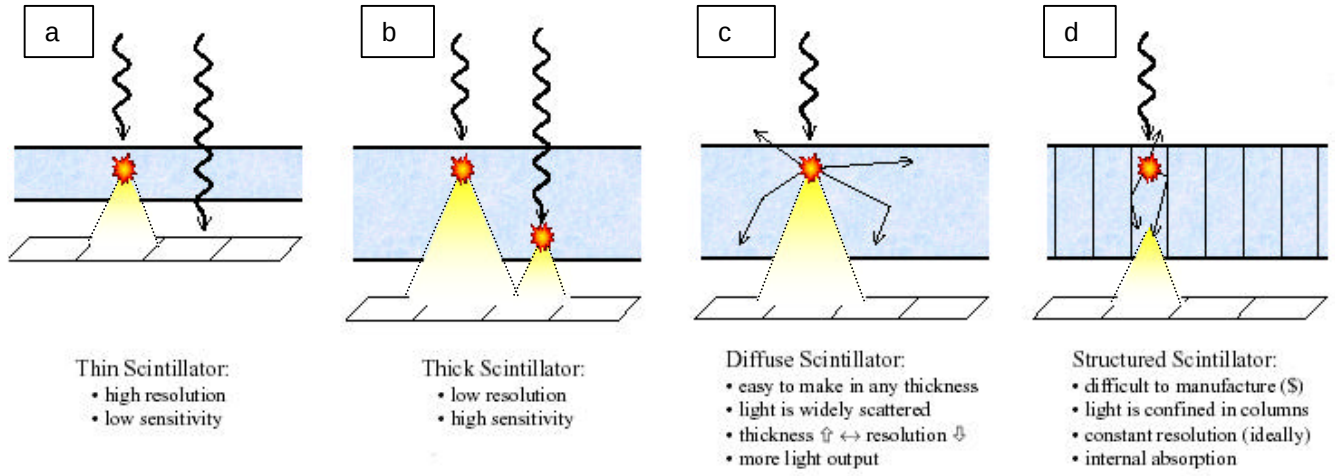

Fig. 5. (a,b) Scintillator detectors: resolution versus sensitivity tradeoff,
(c,d) Diffuse scintillator versus structured scintillator [10].

2. Test matrix

Within this work different vendors of on-line digital X-ray imaging systems were contacted to participate at an on-site evaluation of their system(s) at the SCK CEN hot laboratory for Non-Destructive Post Irradiation Examination (ND-PIE) of fuel rods. If a system could not be made available on-site, tests were performed at other locations using a dummy fuel rod and a system set-up as close as possible to the set-up of the SCK CEN installation. Four systems did participate in the feasibility study:

- a Gd_2O_2S:Tb-scintillator coupled to a CCD-camera with a tapered fiber optic plate,
- a CsI:Tl-scintillator coupled to a photodiode array,
- a ZnS:Cu & Gd_2O_2S:Tb-scintillator coupled to an intensified CCD-camera with reflecting mirrors,
- and a CsI:Tl-scintillator coupled to a CCD-camera with an image intensifier.

Notice that all the systems are on-line indirect-conversion types. Also notice that the systems set at our disposal are not always the vendors' best technical solution for our application at that time. Due to

availability or other practical reasons these systems could not always be evaluated. Beside these four systems also a laser film digitizer was evaluated.

The criteria to evaluate the systems are image quality, integration in the existing hot cell[7] infrastructure, durability and cost price (Table 1). For the image quality a simulation fuel rod is fabricated to evaluate the overall resolution performance of the different digital detectors towards the silver-halide film in a situation comparable to the real X-ray imaging of a fuel rod. The resolution performance of the digital systems is not evaluated as an absolute quantified parameter following a norm, but relatively towards each other according a visual evaluation which determines the smallest object visible with the system. Sensitivity[8], contrast[9] and noise[10] are not evaluated separately as they all determine the overall image resolution performance. A lack of sensitivity or contrast, or an increased noise level will deteriorate the overall image resolution performance of the system. The conditions for a system to succeed in the image quality criteria is to approach the silver-halide image quality. Besides the image quality the integration of the system in the existing hot cell is an important factor as it is difficult, expensive and time consuming to modify any structure of the cell. Thus, only limited space is available for the installation of the detector. Durability is also used as criteria to ensure that financial investment and maintenance are kept to a minimum in the future. And of course the initial investment is also taken into account.

Table 1
Test matrix and criteria

On-line digital X-ray detectors (indirect -conversion systems)				Criteria			
	System Scintillator	Signal support	Digital detector	Image quality	Integration	Durability	Cost price
1	Gd_2O_2S:Tb	Tapered fiber optic plate	CCD-camera	Overall resolution performance should approach silver-halide image quality	Limited installation space	Reduced future investment and maintenance	Low initial investment
2	CsI:Tl	/	Photodiode array				
3	ZnS:Cu & Gd_2O_2S:Tb	Reflecting mirrors	Intensified CCD-camera				
4	CsI:Tl	Image intensifier	CCD-camera				

3. ND-PIE X-ray system for fuel rods at SCK CEN

The objective of the non-destructive X-ray examination is to show the internal condition of the fuel rod after irradiation. In general terms, the radiography is intended to provide information on dimensional changes of the fuel stack length, displacement and factures in the pellets, important

[7] Hot cell: infrasctucture for high radioactive material examination. The infrastructure consist of different layers of protection against radiation and contamination: concrete or lead walls against the gamma and beta radiation and an airclosed underpressered box preventing exterior radioactive contamination. Lead glass protection and master slave manipulators make the handling of radioactive materials and measurement instruments inside the hot cell possible.

[8] Sensitivity of a digital detector is the performance to convert the X-ray pattern into an image with enough information per digital pixel to create an acceptable image quality.

[9] Contrast is the capability of a system to differentiate between different materials and different thicknesses of materials

[10] Noise is directly related to the sensitivy of a system (low sensitivity will result in more noise) but also to the physical or electronical characteristics of the system.

density changes in the fuel material, state of the inter-pellet gaps, plug welding and so on (Figure 6). Full size commercial fuel rods up to four and half meter length can be measured.

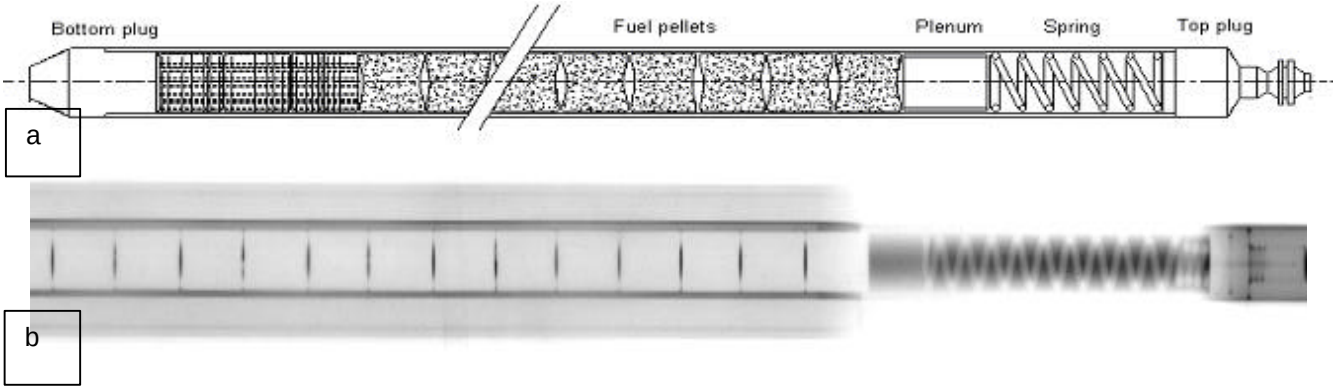

Fig. 6. (a) A general schematic view of a fuel rod, (b) an example of an X-ray image of a part of an irradiated fuel rod.
Fuel pellets, inter-pellet gaps, plenum, spring and the internals of the top plug are clearly visible.

The X-ray examination is performed on a metrology bench equipped to scan the fuel rods with a 420kV tube voltage X-ray source (Figure 7), using high sensitive silver-halide films with lead screens in roll-pack formation. To acquire an X-ray image both fuel rod and film are moved slowly and continuously under the X-ray source. The film speed is increased by a constant speed factor towards the fuel rod speed (typical 0.2mm per second) in order to compensate for the divergence of the X-ray bundle. Depending on the height position of the X-ray source different speed factors and thus different image enlargements are possible. Instead of a continuous movement of the film and fuel rod acquisition can also be done in step mode.
To decrease the exposure of the film due to gamma radiation coming from the fuel rod itself a lead shielding with a 10mm collimator is placed between the fuel rod and the silver-halide film.
As a fuel rod has a circular cross-section, less X-rays will be absorbed in the circular edges of the fuel rod causing a local excessive exposure of the film. Therefore a thickness equalization correction is applied with a parabolic shaped copper attenuator creating a homogeneous X-ray flux[11] all over the circular cross-section onto the film (Figure 7-8).
Since the fuel rod is build up materials with a large difference in attenuation coefficient (Figure 6: empty plenum, inconel spring, very dense fuel, zircalloy tube and plugs) different energy settings are used to scan the different parts of the fuel rod. Low energy X-rays up to 200keV[12] are used for the plenum, spring and plugs, and high energy X-rays up to 400keV are used for the fuel pellets. Notice that these settings and other parameters like scanning speed and tube current are studied and optimized within this work.
As shown in Figure 7 the space available for the positioning of a digital X-ray detector below the collimator is very limited. The space under the collimator is accessible through the concrete floor of the hot cell.

[11] Radiation flux or fluence rate: is the quotient of the number of particles incident on a sphere during a time interval, towards the cross-sectional area of the sphere and the time interval. [13]
[12] The X-ray energy mentioned is always the maximum energy of the X-ray spectra, corresponding to the tube voltage setting. For example, 420kV tube voltage setting produces an energy X-ray spectrum with a maximum energy of 420keV. The average X-ray energy is always lower and rougly about 1/3 of the maximum X-ray energy.

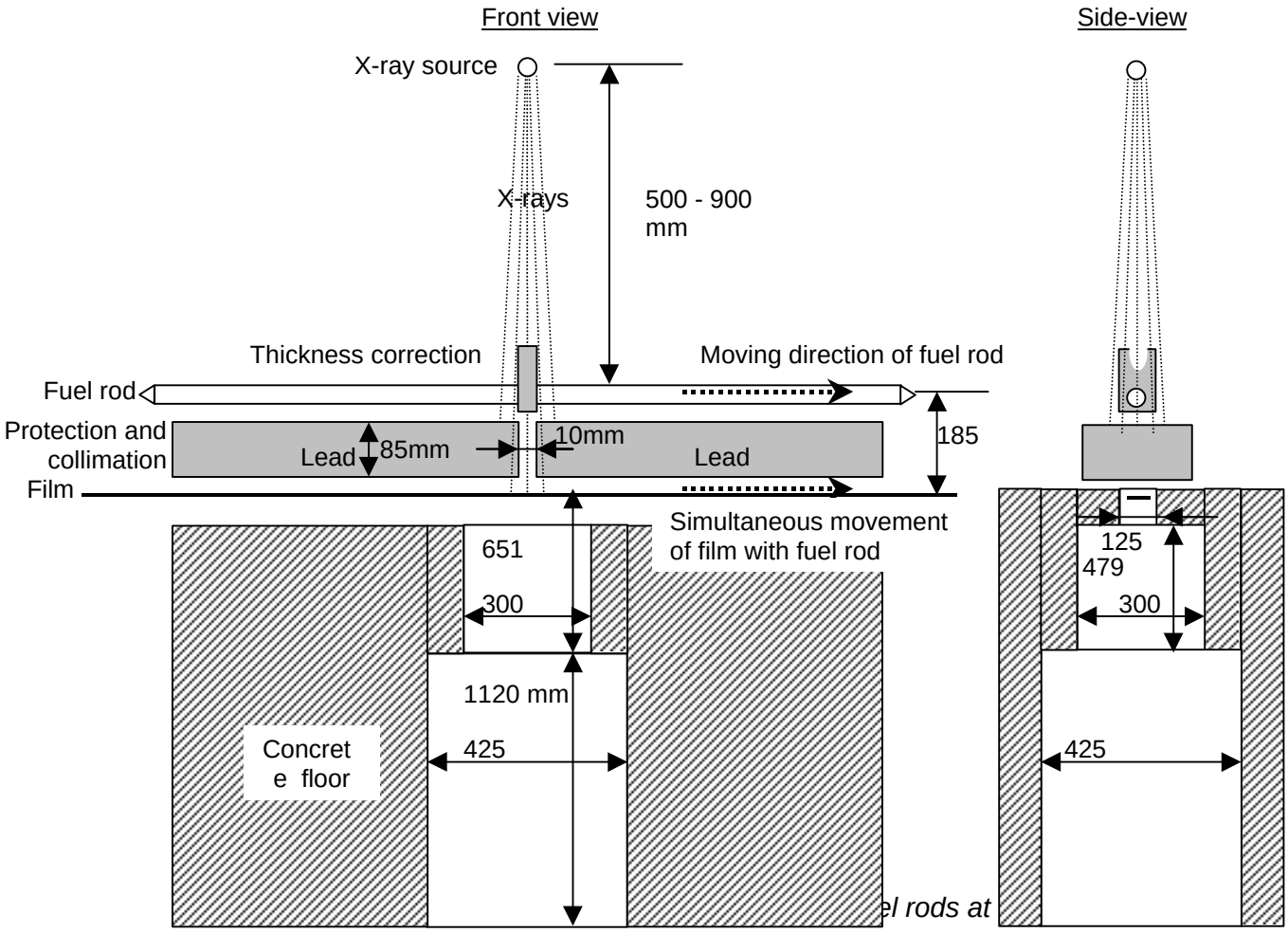

Table 2 gives an overview of the most important characteristics of the ND-PIE X-ray system**.** Film unsharpness is caused by secondary electrons and photons created in the emulsion layer and is quantified as the transition zone for a sharp edged object (Figure 9). Without this transition zone a sharp edged object would be imaged as perfectly sharp. Notice that film unsharpness up to 0.2mm is interpreted by the human eye as an ideal sharp boundary. The geometrical unsharpness is the penumbral shadow at the edge of an object caused by the finite size of the focal spot (Figure 10) and is calculated as:

$$U_g = FSS\frac{FRFD}{FSFRD} \qquad [18]$$

Notice that the geometrical unsharpness is the main contributor to the system unsharpness. So, the resolution performance of the system is mainly deteriorated by the geometrical unsharpness.
The image enlargement is calculated as:

$$IE = \frac{FSFRD + FRFD}{FSFRD}$$

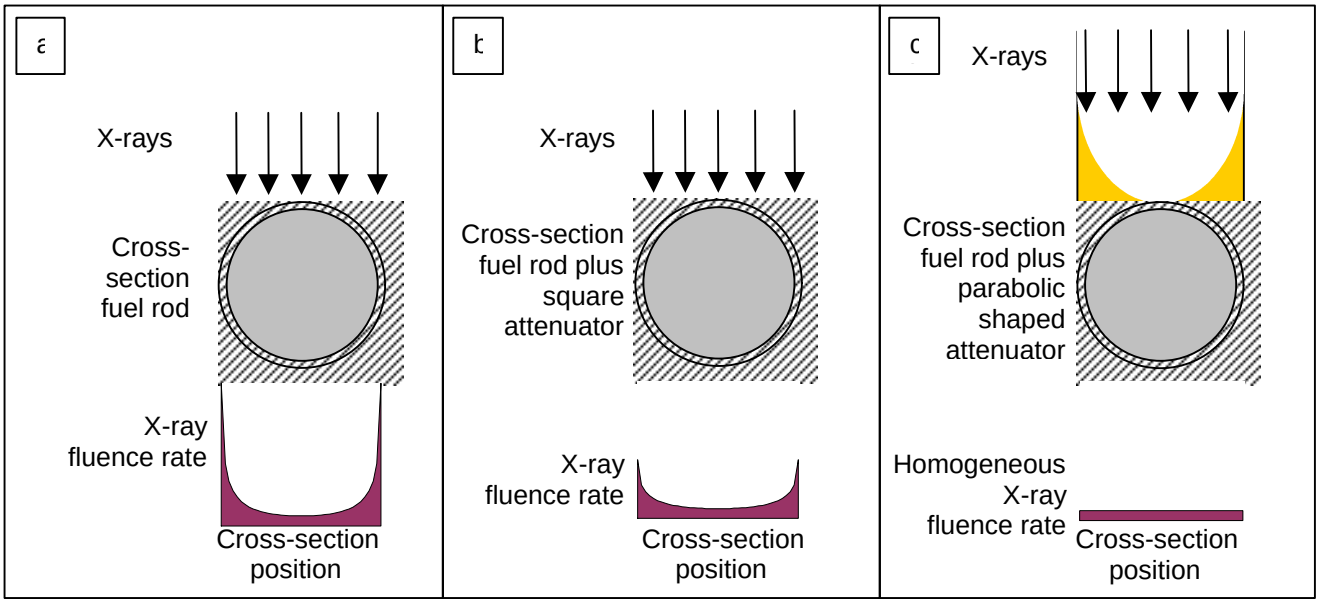

Fig. 8. (a) No thickness equalization correction applied. Overexposure at the edges of the cross-section. (b) A square shaped copper attenuator is insufficient to remove the overexposure, as the attenuation coefficient[13] for copper is less than for nuclear fuel. (c) A parabolic shaped copper attenuator provides a homogeneous X-ray fluence rate.

Table 2
Main characteristics of the ND-PIE X-ray system at the SCK CEN

X-ray source [15]	
Maximum tube voltage	420kV
Maximum tube current at maximum tube voltage	4mA
Focal Spot Size[14] *FSS*	3.3mm
Emergent beam angle[15]	40°
Inherent filtration[16]	7mm Be
X-ray film [16]	
Emulsion	Double sided coating of cubic shaped silver-halide grains
Grain size	Fine
Intensifying screen	0.027mm Pb double sided
Packaging	Daylight rollpac
Film unsharpness U_i	0.2mm [17]
Geometrical set-up (Figure 7)	
Focal Spot – Fuel Rod Distance *FSFRD*	465mm – 950mm
Fuel Rod – Film Distance *FRFD*	185mm fixed
Geometrische unsharpness U_g	1.3mm – 0.6mm
Image Enlargement *IE*	1.40 – 1.19

[13] (Total linear) attenuation coefficient: is the probability per unit length for the removal of a photon (gamma or X-rays) out of the radiation bundel due to interaction with material [14].
[14] Focal spot size reported along the European Norm EN12543. The focal spot size is the dimension of the area from which the X-rays are emitted out of the X-ray tube.
[15] Angle under which the X-ray bundle diverge from the focal spot out of the X-ray tube window.
[16] The inherent filtration removes mainly low energy rays and is due to the interaction of the X-rays with construction components of the X-ray tube itself (like the anode, glass tube, output window,...) and is expressed in an equivalent thickness of Be-filter [2].

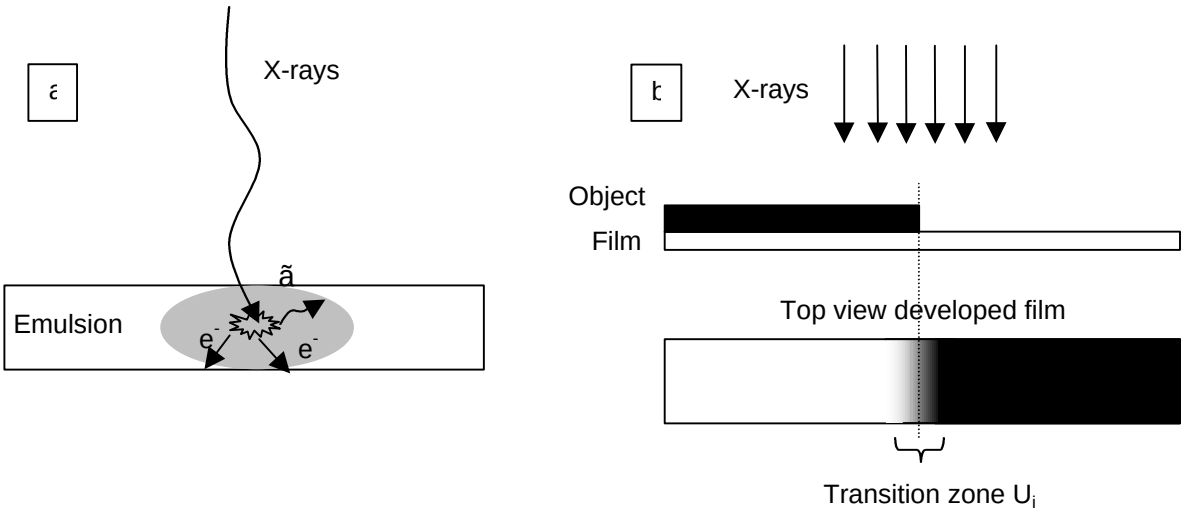

Fig. 9. Film unsharpness. (a) The interaction of the X-rays with the film is spread over a certain distance due to secondary electrons and photons causing an unsharpness in the image. (b) This film unsharpness causes a gray transition zone seen when imaging a sharp edged object.

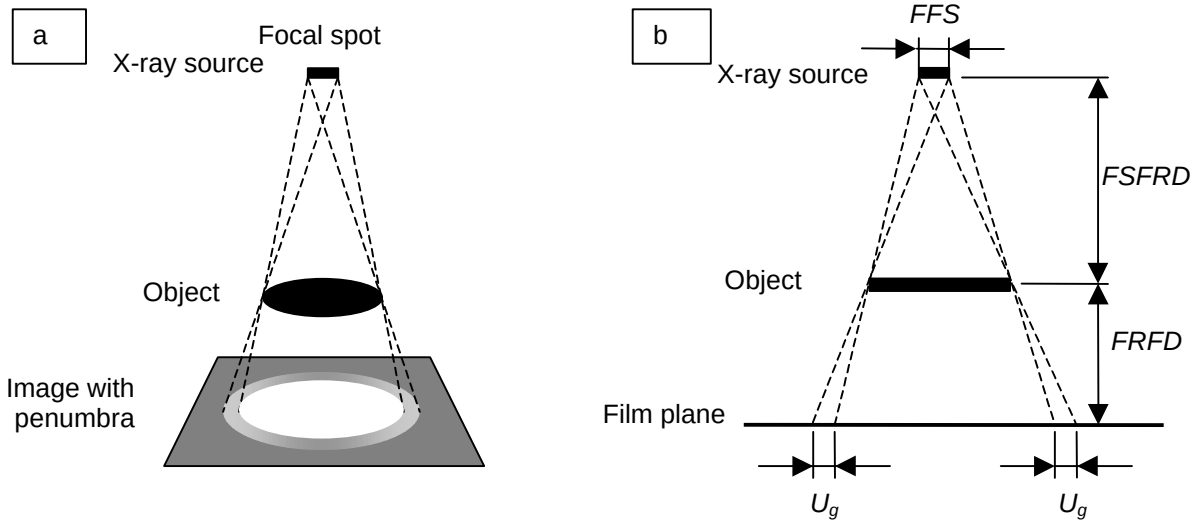

Fig.10. Geometrical unsharpness, (a) demonstration of the penumbra and (b) the determination of U_g.

4. Methodology and technical properties of the evaluated digital X-ray detectors

4.1. System 1: Gd_2O_2S:Tb-scintillator coupled to a CCD-camera with a tapered fiber optic plate

Gadolinium Oxysulfide doped with Terbium (Gd_2O_2S:Tb), or also called Gadox or P43, is a very efficient scintillator in terms of light output per incident X-ray. In addition, its high atomic number and density of 7.3g/cm^3 makes it an efficient absorber of X-rays. Its main disadvantage is that it is manufactured as a compressed powder with particle sizes ranging from 2.5 to 25µm [24], which mean that any light generated by X-rays is scattered and diffuses before it is intercepted by the light detector. Thick Gd_2O_2S:Tb screens, which are needed for the absorption of high energy X-rays of

400keV, have for that reason a limited image resolution. [10]. The scintillator of the evaluated system has an effective field of view of 20mm by 15mm, which is an ideal size for the 10mm collimator of our X-ray system. Along specifications the detector is optimized for tube voltage applications of 10 to 100kV [20], which can cause some lack of efficiency for our application up to 400kV.
The Gd_2O_2S:Tb scintillator is coated onto a tapered Fiber Optic Plate (FOP), which acts as guidance for the fluorescence light towards the digital CCD-camera. The FOP has a multi-fiber construction that bundles single fibers of several micrometers in diameter. Each single fiber consist of a core glass conveying light, a clad glass covering the core glass and an extra absorbent glass in between the fibers absorbing light leakage from the core [19]. As the scintillator has a larger surface ($20x15mm^2$) than the CCD-surface ($8.8x6.6mm^2$) the FOP is tapered towards the CCD with a 2.27 factor in order to have a good fitting (Figure 11). Notice that the presence of the FOP creates a radiation shielding for the CCD-camera, as it is capable of absorbing some of the radiation. Otherwise, high radiation doses can deteriorate the transparency of the glass fibers.
A CCD is a complex semiconductor micro-electronic circuit, which makes it susceptible for radiation damage. The use of an angle FOP can keep the CCD out of the radiation bundle, but is not used for this evaluation. The surface of the CCD is composed of thousands of discrete silicon-based compartments or digital pixels. Incident light generates electron-hole pairs which can be collected and accumulated in a potential well. Each potential well or pixel can be integrated over a certain time before it is electronically read out. The total amount of integrated charges is proportional to the product of the light intensity and the integration time. The complete charge pattern over all the potential wells of the CCD corresponds to the fluorescence image. The number of pixels in the evaluated CCD is 768 by 493 pixels with an actual size of about 12µm. The effective pixel size[17] of the detector, taking into account the enlargement factor of the tapered FOP, is about 27µm. Which means that for a normal fuel rod image acquisition where the image size on the detector is about 10mm (size collimator width) by 12mm (size fuel rod diameter multiplied by an enlargement factor of 1.25) about 370 pixels by 444 pixels will be used. In combination with the tapered FOP and the Gd_2O_2S:Tb scintillator the overall detector resolution is estimated at 43µm [20] for applications up to 100kV tube voltage.
A demerit of the used CCD-camera is that no digital output is present. Instead, the digital image is converted to an analog output signal, in order to view the images on a television monitor. Via this way around the analog output signal is than read in through a special controller which again converts the analog image into a digital image using a 10-bit converter and sends it to a personal computer. These extra conversions can introduce noise and deteriorate the image quality of the original digital CCD-image. The controller has different image processing functions like on-chip integration, image accumulation, image averaging, image zoom, background subtraction and edge enhancement masking.
The evaluated system is presented in Figure 12, together with its physical dimensions. Due to its relative small dimensions the detector can easily be mounted through the hot cell floor under the existing collimator where normally the film is positioned (Figure 7).
The price of the detector including the controller is about € 25000,-.

[17] The effective pixel size is the actual pixel size of the digital detector matrix (for example CCD or photodiode matrix) multiplied by the enlargmentfactor of the detector (for example tapered fiber optic plate or optical lens).

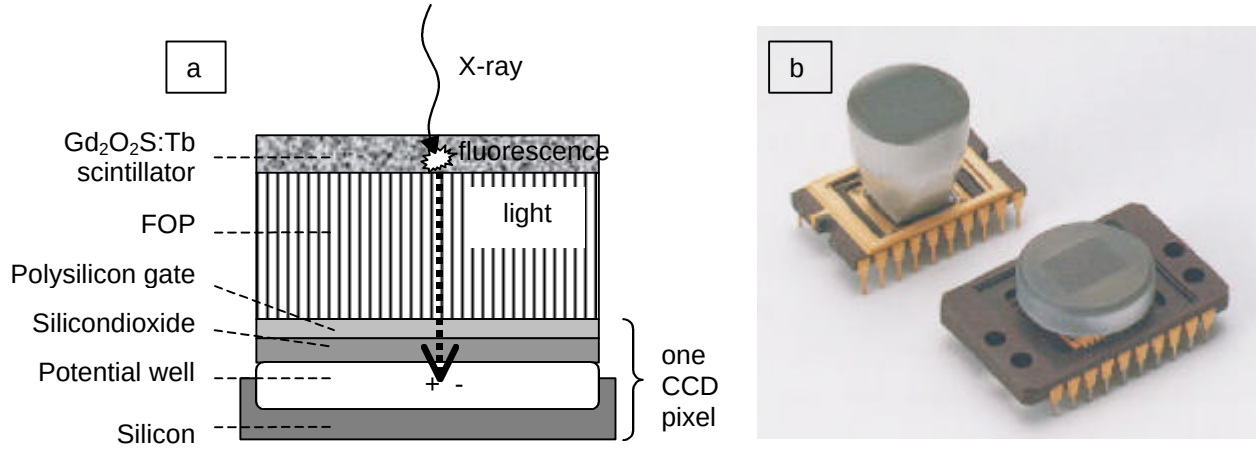

Fig. 11. (a) The schematic view of a scintillator coupled to a CCD-pixel with a FOP. (b) Example of FOP mounted on a CCD-camera chip. Left top is an example of a tapered FOP [21].

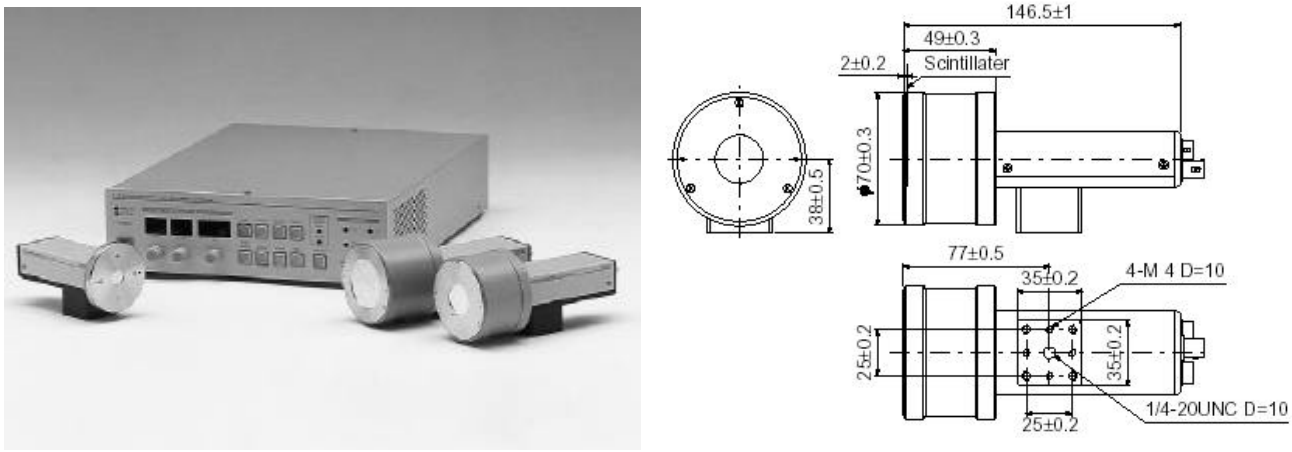

Fig. 12. The evaluated Gd_2O_2S:Tb-scintillator coupled to a CCD-camera with a tapered fiber optic plate [20].

4.2. System 2: CsI:Tl-scintillator coupled to a photodiode array

Cesium Iodine doped with Thallium (CsI:Tl) can also be used as a scintillator material for X-ray detection and imaging. The CsI:Tl material used in this detector is a structured material, build up prismatic crystals (Figure 13). In comparison with the compressed powder materials like Gd_2O_2S:Tb the prismatic material offers advantages like: better spatial resolution as the light is guided by the prisms, more uniform response as the prisms can be grown in a uniform diameter and better light output as the light is not diffused even for thicker scintillators needed for energies up to 400keV [19]. The scintillator of the evaluated system has an active area of 120mm by 120mm [23], which is large compared to the fuel rod image size of 10mm by 12mm. So, only a small amount of the useful detector area is used for imaging which is not favorable for the final image resolution.

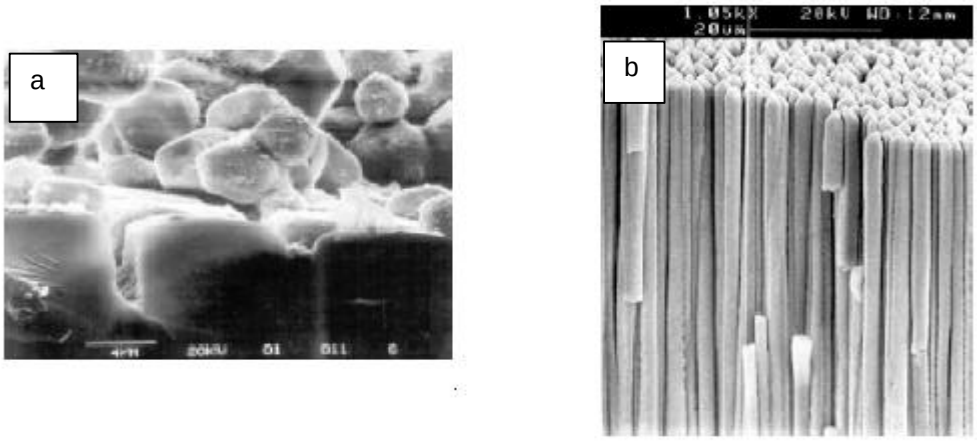

Fig. 13.(a) An example of a compressed powder scintilllator like Gd_2O_2S:Tb, (b) a prismatic CsI:Tl-scintillator [22].

The scintillator is optical coupled to a two dimensional detector matrix where pixels are made up photodiodes sensitive to fluorescence light (Figure 14). The photodiodes are made of amorphous Si semiconductor material in a p-n junction[18] configuration. When light interacts in such a semiconductor p-n junction charges will flow through the junction and will be stored in the pixel . Analog to the CCD the complete charge pattern over the photodiode matrix corresponds to the fluorescence image. The number of pixels of the evaluated system is 2400 by 2400 pixels with an actual and effective size of 50µm. This results in 200 pixels by 240 pixels for a typical fuel rod image size of 10mm by 12mm. Although the total number of pixels of the system is large, only one-tenth is used for the effective imaging of the fuel rod. The overall detector resolution of the photodiode matrix in combination with the CsI:Tl prismatic crystal is estimated at 125µm [23]. Although the prismatic CsI:Tl scintillator has a better intrinsic resolution than the compressed powder Gd_2O_2S:Tb scintilllator, the overall detector image resolution is worse compared to the detector discussed in paragraph 4.1. This can be explained by the fact that the pixel size for the photodiode array is much larger compared to the CCD-camera in spite of the larger number of pixels.
In contrast to the CCD-camera the photodiode detector provides a 12-bit digital image output which can be transferred directly to a personal computer through a frame grabber board. It is advisable to protect the electronic control of the photodiode detector from the radiation field for long-term applications at X-ray energies.
The CsI:Tl photodiode detector evaluated in this work is represented in Figure 15, together with its dimensional properties. As the flat panel detector is too large for the upper area the nearest to the collimator (where normally the film is situated), it was installed 180mm lower in the 300mm by 300mm square section (Figure 7). Notice that the larger distance between the fuel rod and the detector increases the geometrical unsharpness by a factor 2, deteriorating the image resolution.
The price of the evaluated CsI:Tl photodiode detector is about € 50000,- , the most expensive of the four detectors tested except for the laser film digitizer which costs about € 75000,-.

[18] P-doped material has impurities creating valences for electrons in the material, also called holes. N-doped material has impurities creating free electrons in the material. When p- and n-doped materials are connected the material will behave in a particular way: current will flow readily in one direction (forward biased) but not in the other (reverse biased), creating a basic diode. In a particular configurations the diode will act as a photodiode and will be able to convert light into current.

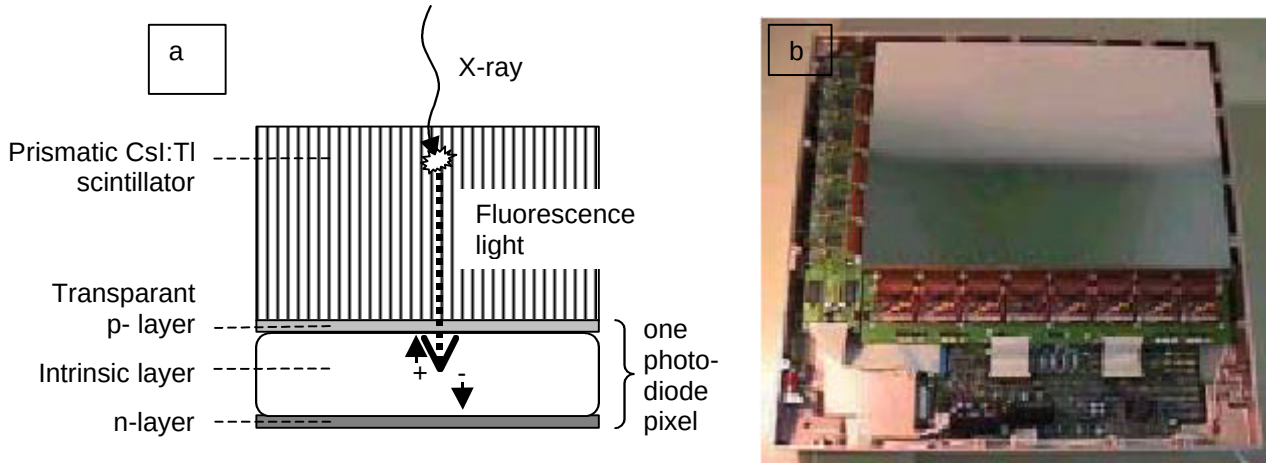

Fig. 14. (a) The schematic view of a prismatic CsI:Tl scintillator coupled to a photodiode pixel. (b) Example of scintillator mounted on a photodiode array with the read out electronics. [22].

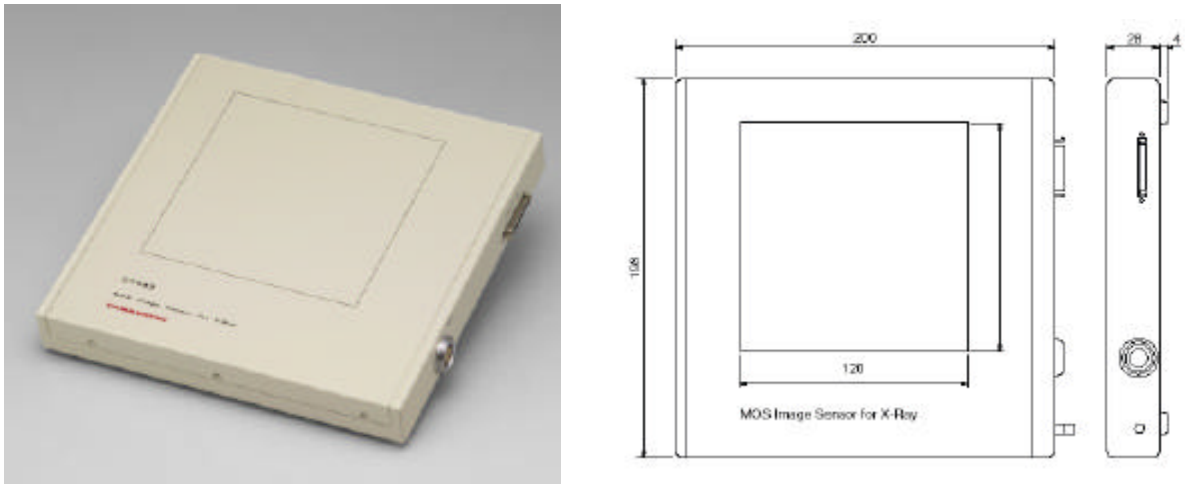

Fig. 15. The evaluated CsI:Tl-scintillator coupled to a photodiode array [23].

4.3. System 3: ZnS:Cu and Gd_2O_2S:Tb-scintillator coupled to an intensified CCD-camera with reflecting mirrors

Instead of having a physical coupling of the scintillator to the CCD, optical mirrors and a lens are used to project the image onto the CCD-camera (Figure 16). These systems have the advantage that scintillators can easily be exchanged. Two types of scintillator materials were tested: Gd_2O_2S:Tb (see § 4.1) and Zink sulfide doped with copper (ZnS:Cu). The ZnS:Cu screen has a higher intrinsic efficiency for converting X-rays into light in spite of the lower mass density of 4.1g/cm^3 [24]. The larger grain sizes ranging from 30 to 40µm [24] can deteriorate the image resolution.

The optical mirrors are placed in such a way that the CCD-camera is kept out of the X-ray bundle in order to minimize any radiation damage to the electronic components. As rear surface mirrors[19] are used image resolution can deteriorate. The optical properties of the lens are optimized to have an optimal use of the CCD-pixels in function of a typical fuel rod image size of 10mm by 12mm. An image dimension of 20mm by 15mm is projected over the 774 by 580 pixels of the CCD-matrix [25], resulting in an effective pixel size of about 26µm.
Since the optical light collection efficiency of the lens is very low an intensified CCD-camera is used. The build-in intensifier is a very compact second generation image intensifier using a micro channel plate to multiply the photo-electrons [26] (Figure 16). The image intensifier is an evacuated tube with a photocathode entrance window. When the luminescent light strikes the cathode, photo-electrons are emitted and accelerated over a potential field towards the micro channel plate.

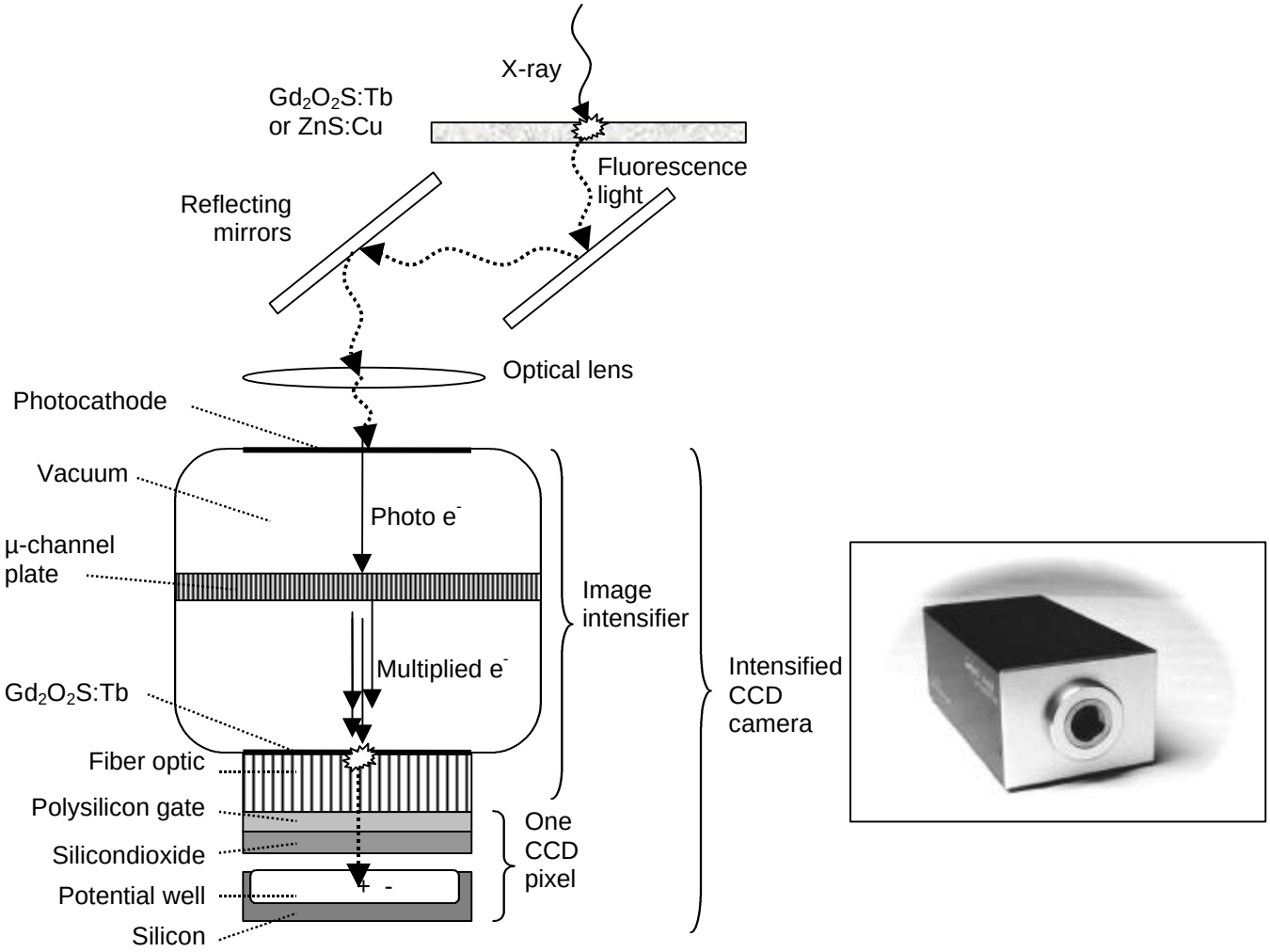

Fig. 16. Schematic view of a scintillator optical coupled with reflecting mirrors to an intensified CCD-camera.On the right a picture of the intensified CCD-camera used in the evaluation [25].

[19] When light reflects off of a rear surface mirror, the light first passes through the glass substrate, resulting in reflection losses, secondary reflections, and a change in apparent distance. First surface mirrors avoid this by aluminizing the front, and coating it with a thin protective SiO coating to prevent oxidation and scratching.

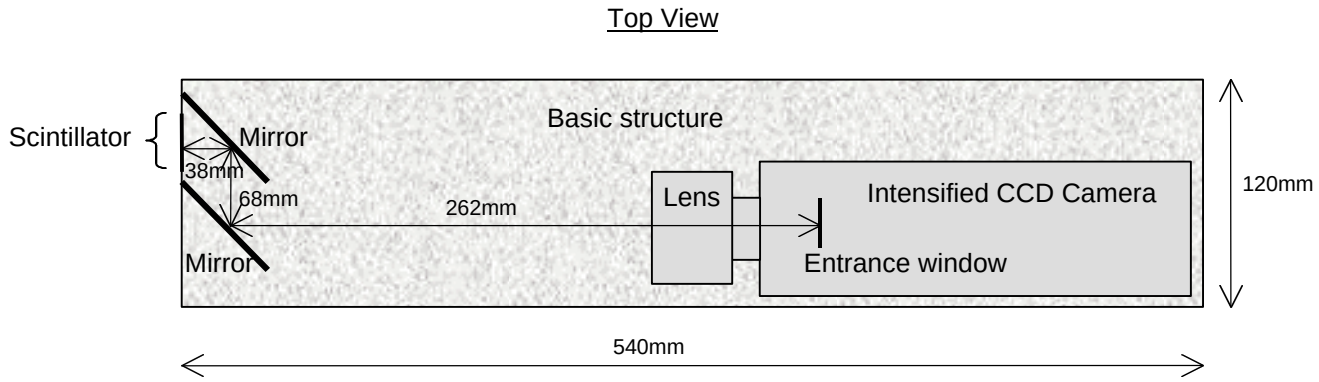

Fig. 17. Dimensional properties of the optical coupled scintillator with reflecting mirrors and intensified CCD-camera, as installed in the hot cell for evaluation.

The micro channel plate consists of a thin disk (<1mm thick) of honeycombed glass with a resistive coating, across which a high potential field is set. An electron entering a honeycomb channel will initiate an electron avalanche. The multiplied electrons are than projected towards a fluorescence Gd_2O_2S:Tb screen on a fiber optic exit window. This fiber optic window, on which the intensified image is projected, is optically coupled to the surface of the CCD-matrix. By changing the potential field over the micro channel plate the gain of the image intensifier is controlled. The intensified CCD-camera has a 10-bit digital output which can be read into a personal computer.
The dimensions of the detector were configured to fit into the upper area under the collimator where normally the silver-halide film is situated (Figure 7, 17).
The price of the digital X-ray system inclusive the controller is about € 25000,-.

4.4. System 4: CsI:Tl-scintillator coupled to a CCD-camera with an image intensifier

Notice that these kind of relatively large analog image intensifiers (Figure 18) are being used in different domains since 1948 [27]. The analog image produced can be seen on a television monitor making use of an analog camera. Nowadays the analog output is digitized with a CCD-camera.
At the entrance window of the image intensifier a prismatic structured CsI:Tl scintillator is coupled to the photocathode (Figure 19). The principle of this large image intensifier [27] is slightly different from the small one used in the intensified CCD-camera discussed in paragraph 4.3. No micro channel plate is used and the photo-electrons are focal accelerated towards the fluorescence screen at the exit window. The intensified output image is achieved, on the one hand, by the acceleration of the photo-electrons, and, on the other hand, by the concentration of the electron flux from the large photocathode area onto the very much smaller output screen area. The output screen is optical coupled to the CCD camera with a first surface mirror and a 35mm objective. The image intensifier has a zoom function which can select a part of the entrance window to be intensified. The zoom function improves the image resolution, but decreases the intensifying performance of the system. As the image size of a fuel rod is small, the largest zoom is used, which results in an active detector area of 120mm by 90mm. As the CCD has a matrix of 756 by 581 pixels, the effective pixel size of the detector is about 157µm [28], which is the largest effective pixel size of all the evaluated digital X-ray detectors. Considering the CCD dimensions of 8.8mm by 6.6mm the actual pixel size of the CCD matrix is about 11.5µm. The overall resolution of the system using the largest zoom is estimated at 360µm [28], which is also probably the worst resolution of the four tested systems. Also notice that in

spite of the largest zoom used, the typical image size of the fuel rod (10mm by 12mm) only uses a small part of the active detector area. When taking images with an image intensifier one always has to prevent an overloading of the detector with non-attenuated X-rays as the intensifier is susceptible to image burn.
A demerit of the used CCD-camera is the absence of a digital output. By use of an external analog-digital converter the analog CCD image is reconverted into a digital image and transferred to a personal computer.
The dimensions of the image intensifier tube available for testing (Figure 18) was too large to introduce in the hot cell area under the collimator. Therefore all tests were performed at the vendors' laboratory. A similar X-ray source up to 420kV tube voltage was used, though with a smaller FSS of 1.6mm [29], which is half the size of the SCK CEN X-ray source. Also the geometrical set-up was altered: a FSFRD and FRFD of 1000mm. The geometrical unsharpness for this set-up is 1.6mm, which is larger than to the SCK CEN set-up. Notice that smaller image intensifier tubes do exist, but were not evaluated on-site due to practical reasons.
The price of a CsI:Tl scintillator coupled to a CCD-camera with an image intensifier is about € 25000,-.

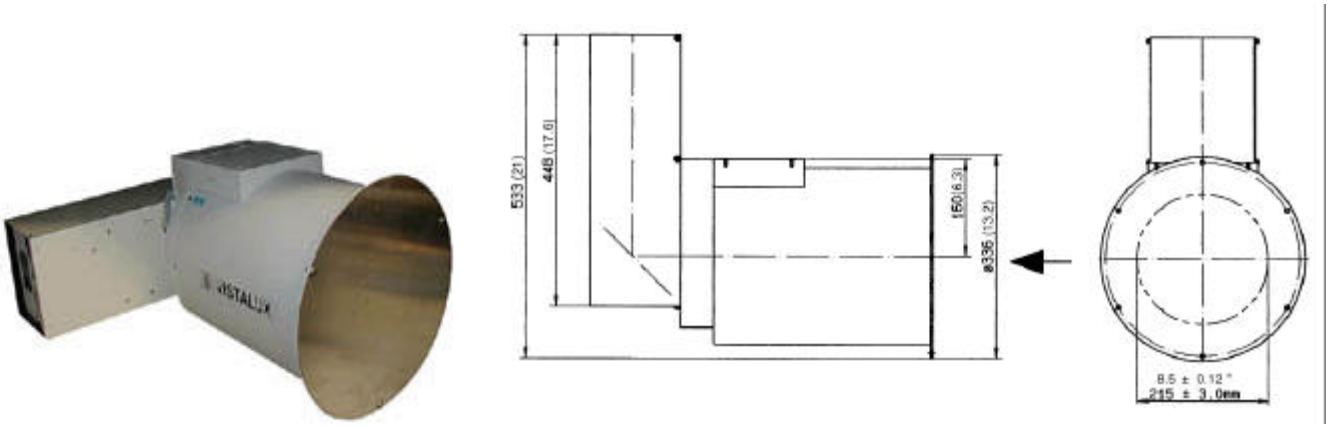

Fig. 18. The evaluated CsI:Tl-scintillator coupled to a CCD-camera with an image intensifier [28].

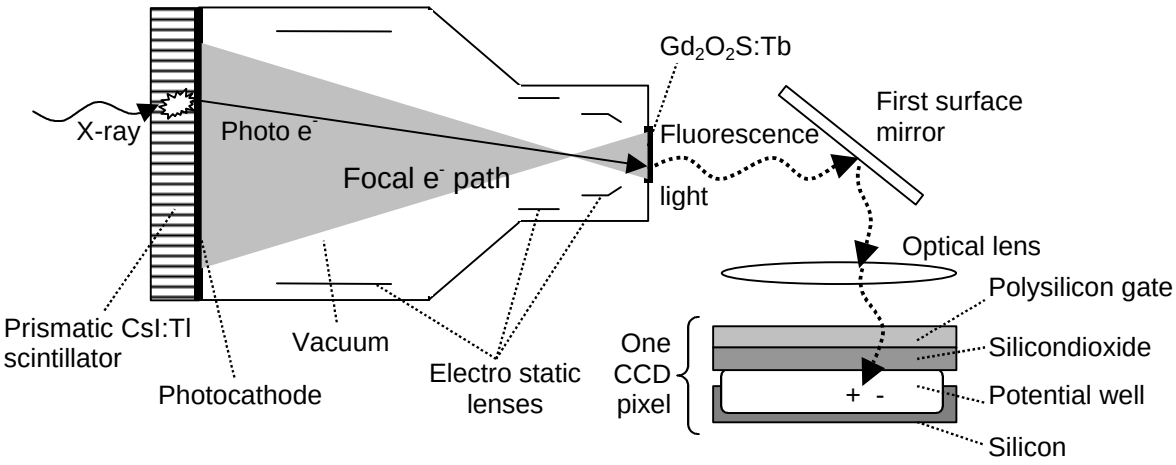

Fig. 19. Schematic view of a CsI:Tl-scintillator coupled to a CCD-camera with an image intensifier.

4.5. System 5: X-ray laser film digitizer

As mentioned in the introduction (§1) the film digitizer is not an on-line X-ray imaging system like the SCK CEN wants to purchase. Nevertheless, the image quality performance of a film digitizer was compared to the on-line digital detectors and the sliver-halide film just to have an idea of the performance of such systems.
There are two basic types of X-ray film digitizers: a CCD digitizers and a laser digitizers. Both techniques measure the optical density of the film based on the light absorption in the film. There is considerable debate about which technology is superior. Laser digitizers seem to be perceived as providing better image quality; CCD digitizers seem to be perceived as offering more value for the money. Certainly, CCD technology has improved considerably over the past few years and today high quality CCD digitizers produce images as good as (or close to as good as) top-of-the-line laser digitizers.
The digitizer evaluated in this work employs a HeNe laser of 632.8nm wavelength, which sweeps across the film by a polygon shaped mirror system[20] (Figure 20). An F-teta lens avoids distortions of the image, by keeping the optical distance of the laser beam unchanged at all spots of the scanned area. The light intensity of the transmitted laser through the film is in simple terms detected by a photomultiplicator tube system[21]. All standard film formats, even rollpacks, can be digitized with an effective pixel size down to 50µm into a 12-bit grayscale image [30].
The price of the evaluated film digitizer is about € 75000,-. Which is even more expensive as the most expensive on-line digital X-ray detector tested. As already mentioned in the introduction, the initial investment for a single installation is too high compared to the purchase of a digital X-ray detector, in case comparable image quality can be achieved.

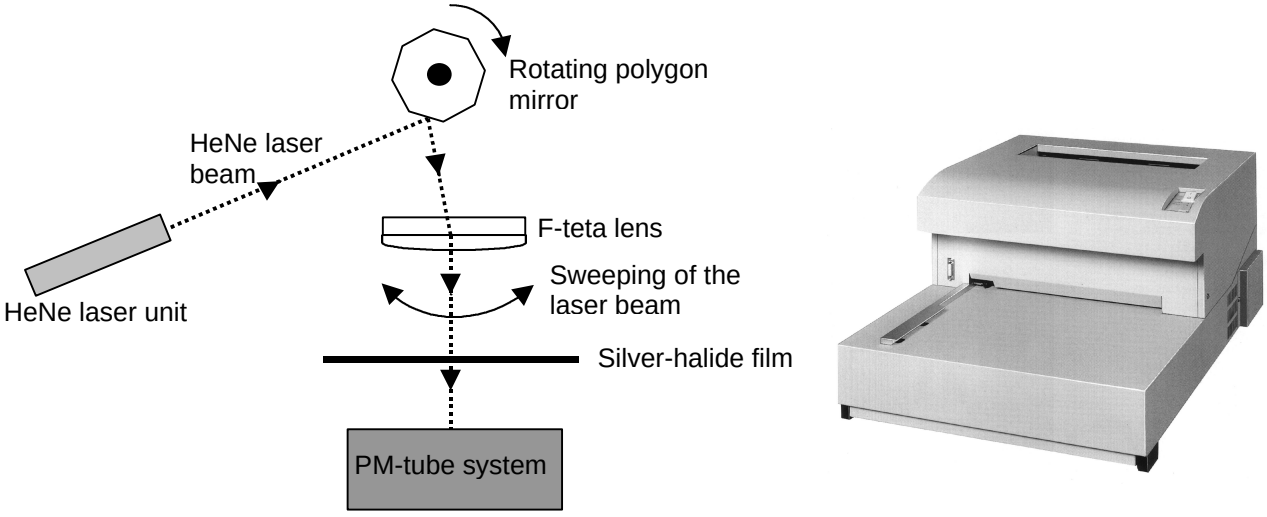

Fig. 20. (a) General principle of a laser film digitizer. (b) Picture of the evaluated X-ray film digitizer [30].

4.6. Round-up and discussion of the technical properties of the evaluated systems

[20] By reflecting a laser beam on a rotating polygon shaped mirror the laser can be send into different directions able to scan an object. These kind of mirror systems are also used intensively in laser printers and copiers.
[21] A photomultiplicator tube (PM-tube) is a vacuum tube which converts detected light into photo-electrons through a photocathode and accelerates and multiplies these electrons in order to achieve an amplified electronic signal at the output, proportional to the intensity of the detected light.

Table 3
Technical properties of the evaluated systems

	System 1	System 2	System 3	System 4	System 5
Scintillator	Gd_2O_2S:Tb	CsI:Tl	Gd_2O_2S:Tb & ZnS:Cu	CsI:Tl	/
Scintillator structure	Compressed powder	Structured	Compressed powder	Structured	/
Scintillator grain size	2.5-25µm	/	2.5-25µm & 30-40µm	/	/
Scintillator efficiency relative to a NaI scintillator	15%	8.5%	15% & 18%	8.5%	/
Light guidance	Tapered FOP	/	Rear surface mirrors	First surface mirror	/
Image intensifier	No	No	Yes	Yes	/
Active area detector	20x15mm^2	120x120mm^2	20x15mm^2	120x90mm^2	/
Detector matrix type	CCD	Photodiode	CCD	CCD	
CCD or photodiode area	8.8x6.6mm^2	120x120mm^2	/	8.8x6.6mm^2	/
Number of pixels	768x493	2400x2400	774x580	756x581	/
Actual pixel size[22]	12µm	50µm	/	11.5µm	/
Effective pixel size[23]	27µm	50µm	26µm	157µm	50µm
Number of pixels for a 10x12mm^2 image[24]	370x444	200x240	385x462	64x76	200 x 240
Overall detector resolution	43µm	125µm	/	360µm	
Energy range	10-100keV	/	/	/	/
Output signal	Analog	Digital	Digital	Analog	Digital
Digital grayscale	10bit	12bit	10bit	/	12bit
Integration in hot cell environment	Yes	Not optimal	Yes	No	/
Possible radiation damage	CCD in radiation bundle	/	/	Image burn	/
Cost price	€ 25000,-	€ 50000,-	€ 25000,-	€ 25000,-	€ 75000,-

[22] Actual pixel size: is the physical dimension of the pixels of the CCD or photodiode matrix. Thus, is the CCD or photodiode area divided by the number of pixels

[23] Effective pixel size: is the dimension of the actual pixel size projected towards the active area of the detector. Thus, is the active area of the detector divided by the number of pixels. The effective pixel size is an important factor for the overal detector resolution.

[24] The 10x12mm image size is the typical size of a fuel rod image. In other words, is the area of the detector which will be used by the fuel rod image.

Table 3 is a résumé of the most important technical specifications of the systems retrieved from technical datasheets and mentioned in paragraphs 4.1 to 4.5. Notice that the most important shortcomings of each system are labeled in a gray background color.
No conclusions can be made concerning the sensitivity of the systems, as no information is available about the thickness of the scintillators and the usable X-ray energy range. Generally spoken one would expect that these systems perform quite well up to 250keV, as most applications using these systems are situated within this energy range. The on-site tests at the SCK CEN will reveal if the systems also can perform up to 400keV (see §5).
Except for System 4, all the other systems seem to have a sufficient detector resolution for our application, as the smallest object visible on the silver-halide film is about 0.2mm. The evaluation on-site will reveal if the resolution of these systems are good enough to approach the image quality of the silver-halide film (see §5).
The CCD of System 1 is susceptible to radiation damage as it is always positioned in the X-ray bundle. Angled FOP's do exist, but where not used in our evaluation. Also the optimal energy range of the system makes it likely not to function very well at higher energies up to 400keV.
System 2 is too large to be positioned near the collimator of the SCK CEN X-ray installation, where normally the silver-halide film is placed (see Figure 7). The geometrical unsharpness increases by a factor 2, as the distance between the fuel rod and the detector has to be increased by another 180mm. Also the price of system 2 is about the double of the other on-line digital X-ray detectors.
System 3 uses rear surface mirrors, instead of first surface mirrors, which will deteriorate the image resolution. Also the sensitivity up to 400keV is questionable as no data is available.
System 4 does not only suffer from an insufficient spatial resolution, also the image burn of the image intensifier can cause problems when the detector is exposed to a high X-ray flux. As the image intensifier does not fit in the hot cell infrastructure, the system was tested at the vendors' laboratory. The geometrical set-up is described in paragraph 4.4. Smaller image intensifiers are available but were not evaluated due to practical reasons.
The pixel size of System 5, which is the laser film digitizer, is probably small enough as the smallest object visible on the silver-halide film is about 0.2mm. Nevertheless, the price is three times higher compared to most on-line digital detectors.

5. On-site evaluation of the digital X-ray systems

5.1. Simulation fuel rod for overall image resolution performance

As already mentioned a simulation fuel rod (Figure 21) is fabricated to evaluate on-site the overall image resolution performance of the different digital detectors towards the silver-halide film in a situation as close as possible to the real X-ray imaging of a fuel rod. The overall resolution of the digital systems is not evaluated as an absolute quantified parameter following a norm, but relatively towards each other according a visual evaluation which determines the smallest object visible with the system. Sensitivity, contrast and noise are not evaluated separately as they all determine the overall image resolution performance. A lack of sensitivity or contrast, or an increased noise level will deteriorate the overall image resolution performance of the system.
X-ray imaging of a fuel rod is performed at two different energy levels. Low X-ray energies up to 200keV for the inconel spring imaging, and high X-ray energies up to 400keV for the fuel pellet imaging. Therefore the simulation fuel rod is composed out of two compartments, one to check the overall image resolution performance for the inconel spring imaging and the other for the fuel pellet imaging. To simulate the inconel and fuel, materials are selected with comparable mass densities in order to have comparable attenuation characteristics for the X-rays. The materials also have to be cheap and easy to work with. To simulate the inconel spring, copper wires are used with different diameters centered in the axial axis of the simulation rod by use of PVC-pellets. The PVC is chosen

for its low interaction probabilities with X-rays. The diameters of the copper wires range from 2.75mm to 0.2mm, making it possible to evaluate the smallest wire visible. So, the overall image resolution performance for the inconel spring imaging is reported as the smallest visible copper wire. To simulate the fuel pellets, lead with 5% antimoon is chosen. Holes are made of different diameters in the axial direction, simulating fuel core melting (Figure 22). The holes range from 2.6mm to 1.0mm in steps of 0.2mm, making it possible to evaluate the smallest hole visible. Also here the overall image resolution performance for fuel pellet imaging is reported as the smallest visible hole in lead.
Besides these two compartments, a third compartment is composed of a sequence of materials with increasing attenuation coefficients for X-rays. The optical density (for silver-halide films) or grayscale value (for digital images) obtained for the different materials represent the overall contrast performance of the system. As already mentioned the contrast is not evaluated within this work as it is indirectly included in the overall image resolution performance (a bad contrast will result in a bad image resolution). The third compartment will only be used for quality assurance purposes.
To have a faithful representation of a real fuel rod, a Zircalloy-4 tube and plugs were used to assemble the simulation fuel rod. So, also the imaging of Zircalloy plugs can be checked.

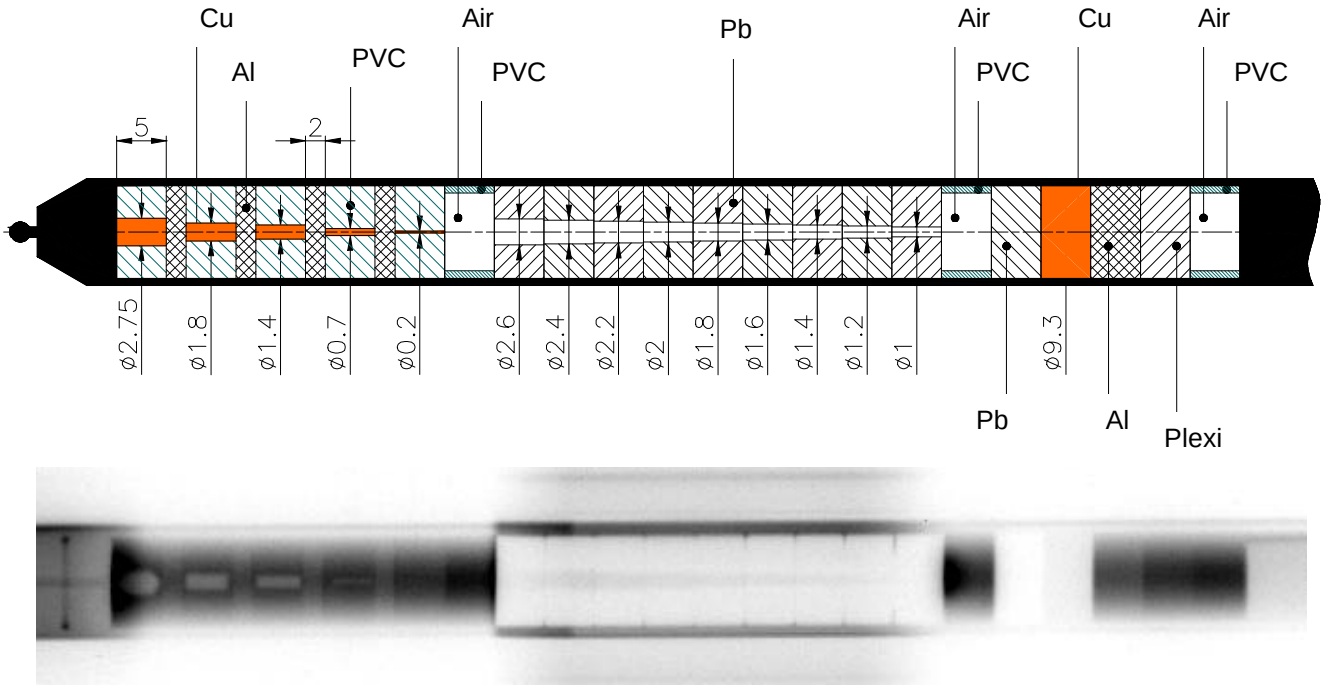

Fig. 21. Composition of simulation fuel rod and its X-ray image. The image has been digitally imported in this document by scanning the original silver-halide film with the laser film digitizer – system 5.

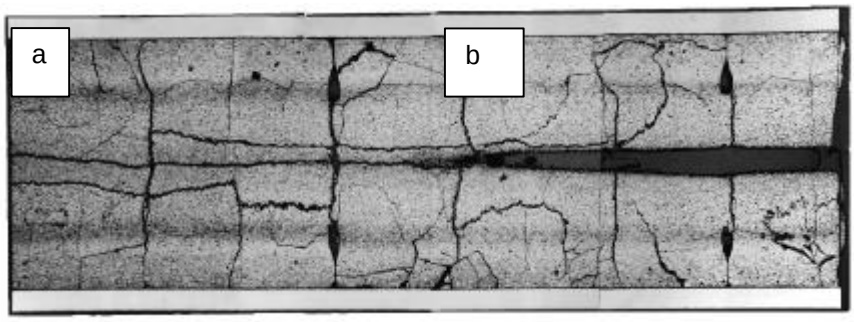

Fig. 22. Example of fuel core melting. (a) Transversal cutting, (b) axial cutting.

5.2. Results overall image resolution performance on-site

The geometrical set-up and X-ray tube parameters for the comparison of the overall image resolution are given in Table 4. Notice that System 2 and 4 have a different geometrical unsharpness, as System 2 could not be placed nearer the fuel rod and System 4 was measured at the vendors' laboratory. Images were optimized for tube voltage, tube current and exposure time until the best image resolution performance was reached. Table 5 summarizes the best achieved simulation fuel rod images for each system.

Table 4

Geometrical set-up and X-ray source parameters for on-site evaluation of the overall image resolution

	System 1	System 2	System 3	System 4	System 5
FSS	3.3mm	3.3mm	3.3mm	1.6mm	3.3mm
FSFRD	740mm	740mm	740mm	1000mm	740mm
FRFD	185mm	365mm	185mm	1000mm	185mm
U_g	0.8mm	1.6mm	0.8mm	1.6mm	0.8mm
Tube voltage for Cu-wires	180kV	180kV	200kV	/	150kV
Tube voltage for Pb-pellets	380kV	390kV	390kV	420kV	390kV
Tube voltage for Zr-4 plug	200kV	180kV	200kV	215kV	200kV
Tube current for Cu-wires	6mA	6mA	7mA	/	4mA
Tube current for Pb-pellets	4mA	4mA	4mA	2mA	4mA
Tube current for Zr-4 plug	6mA	6mA	4mA	2mA	4mA
Exposure time for Cu-wires	100ms	10s	140ms	/	/
Exposure time for Pb-pellets	80ms	10s	5s	/	/
Exposure time for Zr-4 plug	80ms	3s	3.4s	/	/

Table 5
Results overall image resolution performance on-site with simulation fuel rod

	Film	System 1	System 2	System 3 with Gd_2O_2S:Tb	System 3 with ZnS:Cu	System 4	System 5
Cu-wires	0.2mm visible	0.7mm visible 	0.7mm visible 	N/A	0.7mm nearly visible 	N/A	0.7mm visible 
Pb-pellets	1mm visible	2.6mm not visible	1.0mm visible 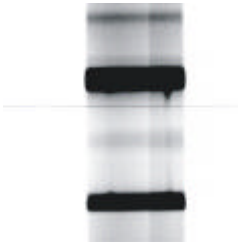	1.0mm visible 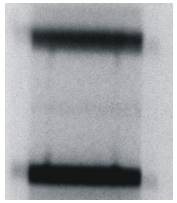	1.0mm visible 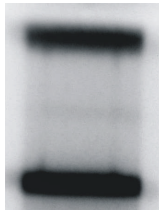	1.0mm visible 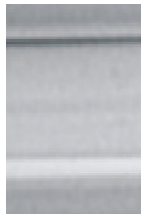	1.0mm visible 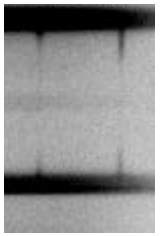
Zr-4 plug		Not as good as film 	As good as film 	Not as good as film 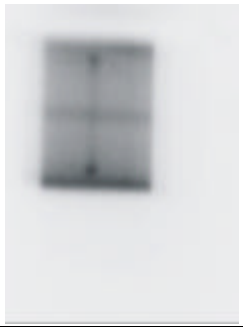	N/A	As good as film 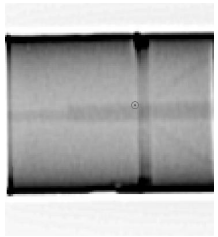	As good as film 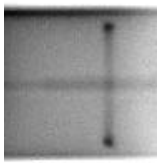

5.3. Discussion overall image resolution performance on-site

The performance of the silver-halide film is taken as reference for the evaluation. The digital systems should approach the film performance as close as possible. The 0.2mm Cu-wire is visible if the source parameters are optimized. A slight change in parameters makes the 0.2mm Cu-wire disappear. So, the resolution of the inconel spring imaging is limited to 0.2mm for the silver-halide film. The smallest hole of 1mm in lead is clearly visible. Probably the resolution for the fuel pellet imaging on silver-halide film is even better as 1mm, but could not be checked as smaller holes in the lead simulation pellets are not present.
For system 1 the Cu-wire of 0.7mm is still clearly visible. Indicating that the resolution for the inconel spring imaging is situated somewhere between 0.7mm and 0.2mm. When looking closer at the image white spots are randomly present due to noise coming from the CCD-chip. A cooled CCD-chip could be a solution to this problem. Above the lead pellets no images could be produced, due to a serious lack of sensitivity for high X-ray energies up to 380keV. An increase of the integration time could be a solution to this problem, but was not possible with the system. Also here a cooled CCD-camera will be needed to reduce the noise during the long integration times. The lack of sensitivity at high energies was already suggested on basis of the technical properties of the system. Unfortunately, it makes system 1 unsuitable for our application.
System 2 has the same performance above the Cu-wires. Unlike System 1 no random noise is seen. The hole of 1mm in lead is visible when increasing the contrast of the image. Unfortunately, serious image non-uniformity gets visible when doing so. The non-uniformity of the images at high energies makes the system not appropriate for our application. Also notice the horizontal blank array of pixels through the image, caused by a damaged photodiode array.
For System 3 the Cu-wire of 0.7mm is nearly visible. Indicating that the resolution for inconel spring imaging is limited to 0.7mm, thus less performative as System 1 and 2. The images have less contrast and sharpness. The lost of sharpness could be caused by the use of the rear surface mirrors. Compared towards the film the image quality is unacceptable for our application.
Unfortunately for system 4, no images are available for the Cu-wires. But looking at the Zr-4 plug image and comparing it with the other systems one would expect an image resolution very near to the silver-halide film. All this, in spite of the bad detector resolution specified by the vendor and the larger geometrical unsharpness during the test. The pixel size (0.157mm) is relatively large but should be no limit as the image resolution of the silver halide film is (0.2mm) and no gain is taken by decreasing the pixel size below the resolving power of the imaging system [2]. Also the 1mm hole in lead is visible and comparable to the film quality.
System 5, which is the film digitizer, can not reproduce the image resolution of the film as the 0.2mm Cu-wire is not visible after digitizing the film.

Conclusions

From the four evaluated on-line digital X-ray detectors only system 4, which is the CsI:Tl scintillator coupled to a CCD-camera with image intensifier, gave a sufficient image quality. System 1 has a serious lack of sensitivity for higher X-ray energies. System 2 shows an image non-uniformity at high X-ray energies, which is unacceptable. System 3 has an image resolution performance which is unsatisfactory for our application.
On the other hand the image intensifiers' dimensions of System 4 are difficult to integrate in the existing hot cell infrastructure. Also the durability of intensifier screens is questionable as they are susceptible to image burn. Smaller image intensifiers easier to integrate are commercial available nowadays.
The initial investment in a film digitizer is too high compared to the purchase of an on-line digital X-ray detector, as comparable image quality can be achieved.

References

[1] U. Zscherpel, Film digitisation systems for DIR : Standards, Requirements, Archiving and Printing, Bundesanstalt für Materialforschung und –prüfung, Berlin

[2] Harold Johns, John Cunningham, The physics of radiology, Charles C. Thomas, 1983

[3] H. Janssens, Chapter V: Quality of the radiological image, Nuclear Medicine Dosimetry, 4th cycle Industrial Engineer Nuclear Energy, Hogeschool Limburg, MD4-5, 1993

[4] D.L.Y. Lee et al., Direct-conversion X-ray detectors using amorphous selenium, Journal of X-ray science and technology, Volume 10, Number 1,2, page 17-36, 2002.

[5] Wei Qian et al., Multiresolution/multiorientation based nonlinear filters for image enhancement and detection in digital mammography, Journal of X-ray science and technology, Volume 10, Number 1,2, page 1-15, 2002

[6] M. Sonoda et al., Computed radiography utilizing scanning laser stimulated luminescence, Fuji Photo Film, Radiology 148, 833-838, 1983

[7] R.E. Green et al., Computed Radiography, Thieme Medical Publishers, Inc., ISBN 0-86577-351-3, 1992

[8] Y. Tateno et al., Computed Radiography, Springer-Verlag, ISBN 0-387-700021-8, 1987

[9] C. Chaussat et al., New CsI/á-Si 17"x17" X-ray flat panel detector providing superior detectivity and immediate direct digital output for general radiography systems, Physics of Medical Imaging 1998, SPIE 3336, 45-55, February 1998

[10] Rad-icon Image Corp, AN07: Scintillator Options for Shad-o-Box cameras, http://www.rad-icon.com/pdf/Radicon_AN07.pdf 2002

[11] Justin M. Henry et al., Solid State X-Ray Detectors for Digital Mammography, SPIE 1995 conference on Medical Imaging.

[12] Amendolia S.R. et al., Comparison of the imaging properties of some digital radiographic systems, Dip. di Fisica dell'Università & INFN, Pisa, Italy, http://workshop2000.physik.uni-freiburg.de/transparencies/marzulli1.pdf

[13] Radiation quantities and units, ICRU Report 33, 1980

[14] K. S. Krane, Introduction Nuclear Physics, John Wiley & Sons Inc, 1988

[15] Pantak Seifert X-ray Systems, Isovolt 420/10, Product Information, No. 2.530.22.00.02, AgfaNDT.com, 25.02.2002

[16] Structurix Film Systems, Radiographic Film Systems, Agfa, http://ndt.agfa.com/BU/NDT/index.nsf/Text/Structurixbrochure2002/$file/Structurixbrochure2002.pdf

[17] Industriële Radiografie, Holografie, Agfa-Gevaert, 21.5220(1275)

[18] Standard guide for radiographic testing, SE94, ASME boiler and pressure vessel code, Section V Nondestructive examination, 1995 edition, july 1

[19] FOS (Fiber Optic plate with Scintillator) for digital X-ray Imaging, Technical Information Feb 1996, Hamamatsu, Cat. No. TMCP9003E01

[20] X-ray CCD Camera C6086 Series, Hamamatsu Data Sheet, March 2001, Cat. No. SICS1042E06

[21] Creating new optical design – Fiber optic plates, Hamamatsu, October 1998, Cat. No. TMCP1005E02.

[22] H.K. Kim, Status and prospect of pixel detectors for radiation imaging, Department of nuclear and quantum engineering, Department of materials science and engineering, Korea Advanced Institute of Science and Technology, http://mulli2.kps.or.kr/nuclear/school2003/presentation/kimhokyung.pdf

[23] Flat Panel Sensor C7942, C7943, Data sheet, Hamamatsu, Preliminary data September 2001, KACCC0137EA.

[24] Applied Scintillation Technology, Phosphors technical summary and usage, http://www.apace-science.com/ast/phosphor.htm

[25] Li-µCam, Digital Intensified CCD Camera, Technical Specifications, Lambert Instruments, http://www.lambert-instruments.com

[26] ICCD Detectors, Course Notes, September 2002, Andor Technology, http://www.lot-oriel.com/pdf/all/erlaeuter_iccd.pdf

[27] Krestel, Erich, Imaging Systems for Medical Diagnostics**,** Siemens/Publicis, ISBN 3-8009-1564-2

[28] Image Intensifier – Television System VISTALUX 9S3-CCD, Specification No. 1.572.15.00.02, Seifert X-ray Technology, 10-07-00

[29] Pantak Seifert X-ray Systems, Isovolt 420/5, Product Information, No. 2.530.41.00.02, AgfaNDT.com, 21.02.2002

[30] Film digitizer Radview FS50, Technical Brochure, Agfa NDT Inc.